

**Subject Areas:**

optics

**Keywords:**

electromagnetic helicity, dichroism, scattering

**Author for correspondence:**

Manuel Nieto-Vesperinas

e-mail: [mnieto@icmm.csic.es](mailto:mnieto@icmm.csic.es)

# Chiral optical fields: A unified formulation of helicity scattered from particles and dichroism enhancement

---

 Manuel Nieto-Vesperinas
 

---

Instituto de Ciencia de Materiales de Madrid, Consejo Superior de Investigaciones Científicas, Campus de Cantoblanco, Madrid 28049, Spain.

We establish a general unified formulation which, using the optical theorem of electromagnetic helicity, shows that dichroism is a phenomenon arising in any scattering -or diffraction- process, elastic or not, of chiral electromagnetic fields by objects either chiral or achiral. It is shown how this approach paves the way to overcoming well-known limitations of standard circular dichroism, like its weak signal or the difficulties of using it with magnetodielectric particles.

Based on the angular spectrum representation of optical fields with only right circular or left circular plane waves, we introduce beams with transverse elliptic polarization and possessing a longitudinal component. Then our formulation for general optical fields shows how to enhance the extinction rate of incident helicity, (and therefore the dichroism signal), versus that of energy of the light scattered or emitted by a particle, or viceversa.

# 1. Introduction

Chiral fields are acquiring increasing attention due to their potential as probes of matter at the nanoscale [1–9], of which life molecules are of paramount importance, or as high information capacity signals in communication channels [8,10–13] with control and transfer of angular momentum, which includes recently developed structured materials and metasurfaces. The conservation of the electromagnetic *helicity* of wavefields (or, equivalently, *chirality* when they are quasi-monochromatic; we shall indistinctly use both terms for such fields) [4,6,14,15] was recently shown [16] to lead to a new *optical theorem* which characterizes the excitation and emission of field helicity -or chirality- by bodies, and that we believe should play a growing relevant role in coming years with the progress of research on applications of twisted light.

In this context, we pointed out [16] that *circular dichroism* (CD) [17–19], i.e. the difference in absorption -or emission- of energy by molecular objects according to the handedness of circularly polarized light (CPL), is a particular case of this optical theorem for scatterers, and hence it does not need to resort to quantum mechanics as usually done in its standard formulation. Thus this phenomenon is just a consequence of the conservation of helicity of electromagnetic fields on scattering.

Different studies have discussed what kind of structures are necessary to produce chiral fields and whether CD requires those objects being chiral. However, some works have recently shown that this effect can be obtained with achiral objects [20]. Moreover, separating the existence of chirality from dichroism effects may be a problem in some observations [21]. Nonetheless no general and unified framework, not limited to particular structures, has been yet established.

In this paper we show that dichroism is not only an effect due to absorption and e.g. fluorescent re-emission by molecules; but it constitutes a property of any scattering interaction, elastic or not, of electromagnetic twisted fields. Thus based on the aforementioned optical theorem for the helicity, we generalize the concept of dichroism and demonstrate how it appears not only with CPL waves, but also with arbitrary chiral optical fields. This allows the design of an illumination that enhances the information content of the scattered signal, overcoming well-known limitations of standard CD detection, like its weak signal or its difficulties with magnetic objects [22].

For comprehensiveness we next present a summary of concepts associated to the helicity and its optical theorem. Then we show how general optical fields, expressed by its angular spectrum of plane waves, may be represented as a superposition of CPL components of right handed (RCP) and/or left-handed (LCP) polarization. This explicitly formulates in a quantitative manner previous descriptions of helicity of general wavefields; and permits us to introduce a class of elliptically polarized hypergeometric beams, as well as their Hermite and Laguerre derivations, which naturally appear when such representation is applied to a Gaussian angular spectrum.

We then establish how the helicity optical theorem, applied to arbitrary fields and to chiral optical beams in particular, leads to a unified generalization of the theory of dichroism. A first consequence of which is *to put forward the way of enhancing either the extinction of helicity and hence the dichroic signal, or the extinction of intensity*. Such configurations and detections are amenable to future experiments.

## (a) The excitation of helicity

Quasimonochromatic fields have a time-harmonic dependence, i.e. their electric and magnetic vectors  $\mathcal{E}$  and  $\mathcal{B}$  are described in terms of their complex representations  $\mathbf{E}$  and  $\mathbf{B}$  as:  $\mathcal{E}(\mathbf{r}, t) = \Re[\mathbf{E}(\mathbf{r}) \exp(-i\omega t)]$  and  $\mathcal{B}(\mathbf{r}, t) = \Re[\mathbf{B}(\mathbf{r}) \exp(-i\omega t)]$ , respectively.  $\Re$  denoting real part. Then the two fundamental quantities we deal with in this work are the *helicity density*,  $\mathcal{H}$ , and the *density of flow of helicity*,  $\mathcal{F}$ , which in a non-absorbing dielectric medium of permittivity  $\epsilon$ , permeability  $\mu$  and refractive index  $n = \sqrt{\epsilon\mu}$  are [6,16]:  $\mathcal{H} = \langle \mathcal{H} \rangle = \frac{1}{2k} \sqrt{\frac{\epsilon}{\mu}} \Im(\mathbf{E} \cdot \mathbf{B}^*)$  and  $\mathcal{F} = \langle \mathcal{F} \rangle = \frac{c}{4nk} \Im(\epsilon \mathbf{E}^* \times \mathbf{E} + \frac{1}{\mu} \mathbf{B}^* \times \mathbf{B})$ .  $\langle \cdot \rangle$  denoting time-average,  $\Im$  meaning imaginary part and  $k = n\omega/c$ . It must be recalled that for these time-harmonic fields  $\mathcal{F}$  coincides with the

spin angular momentum density and is [4,6,15,16]  $k^2$  times the flow of chirality. On the other hand,  $\mathcal{H}$  is  $k^2$  times the chirality. Also, they fulfill the continuity equation [4,6,15,16]:  $\mathcal{H} + \nabla \cdot \mathcal{F} = -\mathcal{P}$ . Where the helicity dissipation on interaction of the fields with matter is represented by  $\mathcal{P}$ .

Let a quasimonochromatic field, whose space-dependent complex representation is denoted as  $\mathbf{E}_i, \mathbf{B}_i$ , illuminates a particle which we consider magnetodielectric and bi-isotropic [23,24], dipolar in the wide sense i.e. if for instance it is a sphere, its magnetodielectric response is characterized by its electric, magnetic, and magnetoelectric polarizabilities:  $\alpha_e, \alpha_m, \alpha_{em}, \alpha_{me}$ , given by the first order Mie coefficients as:  $\alpha_e = i \frac{3}{2k^3} a_1$ ,  $\alpha_m = i \frac{3}{2k^3} b_1$ ,  $\alpha_{em} = i \frac{3}{2k^3} c_1$ ,  $\alpha_{me} = i \frac{3}{2k^3} d_1 = -\alpha_{em}$ .  $a_1, b_1$  and  $c_1 = -d_1$  standing for the electric, magnetic, and magnetoelectric first Mie coefficients, respectively [24,25]. The condition  $\alpha_{em} = -\alpha_{me}$  expressing that the object is chiral. We remark that by *particle* we shall understand small objects such as e.g. atoms, molecules, material macroscopic particles, or quantum dots.

The electric and magnetic dipole moments,  $\mathbf{p}$  and  $\mathbf{m}$ , induced in the particle by this incident field are:

$$\mathbf{p} = \alpha_e \mathbf{E}_i + \alpha_{em} \mathbf{B}_i, \quad \mathbf{m} = \alpha_{me} \mathbf{E}_i + \alpha_m \mathbf{B}_i. \quad (1.1)$$

At any point outside this scattering object, the total field is written as:  $\mathbf{E}(\mathbf{r}) = \mathbf{E}_i(\mathbf{r}) + \mathbf{E}_s(\mathbf{r})$ ,  $\mathbf{B}(\mathbf{r}) = \mathbf{B}_i(\mathbf{r}) + \mathbf{B}_s(\mathbf{r})$ . The subindex  $s$  denoting the scattered, or radiated, field.

The optical theorem that rules the conservation of helicity described by the above mentioned equation:  $\mathcal{H} + \nabla \cdot \mathcal{F} = -\mathcal{P}$ , is [16]

$$-\mathcal{W}_{\mathcal{H}}^a = \frac{8\pi c k^3}{3\epsilon} \Im[\mathbf{p} \cdot \mathbf{m}^*] - \frac{2\pi c}{\mu} \Re\left\{-\frac{1}{\epsilon} \mathbf{p} \cdot \mathbf{B}_i^* + \mu \mathbf{m} \cdot \mathbf{E}_i^*\right\}. \quad (1.2)$$

In the left side of (1.2)  $\mathcal{W}_{\mathcal{H}}^a$  is the rate of dissipation by the particle of the incident field helicity. It comes from the integration of  $\mathcal{P}$  in a volume that contains this body. On the other hand, from Gauss' divergence theorem the terms in the right side of (1.2) arise from the flow of  $\mathcal{F}$  across a surface that contains the particle [16]. The first of these terms represents the *total helicity scattered or radiated* by the object, whereas the second one constitutes the *extinction of helicity* of the incident wave on scattering. This latter extinction term:  $-(2\pi c/\mu) \Re\{-\frac{1}{\epsilon} \mathbf{p} \cdot \mathbf{B}_i^* + \mu \mathbf{m} \cdot \mathbf{E}_i^*\}$  should be used for determining both dissipated and radiated, or scattered, helicity by a dipolar particle in an arbitrary, homogeneous or inhomogeneous, embedding medium. To emphasize this interpretation we recall its analogy with the well-known optical theorem for energies [26]

$$-\mathcal{W}^a = \frac{ck^4}{3n} [\epsilon^{-1} |\mathbf{p}|^2 + \mu |\mathbf{m}|^2] - \frac{\omega}{2} \Im[\mathbf{p} \cdot \mathbf{E}_i^* + \mathbf{m} \cdot \mathbf{B}_i^*]. \quad (1.3)$$

$\mathcal{W}^a$  being the rate of energy absorption from the illuminating wave. In the right side of (1.3) the first term constitutes the total energy scattered by the dipolar object, whereas the second one represents the energy extinguished from the illuminating field, or rate of energy excitation in the scattering object.

Henceforth we remark the analogous role played by the right side terms in both optical theorems (1.2) and (1.3). As is well-known  $(\omega/2) \Im[\mathbf{p} \cdot \mathbf{E}_i^* + \mathbf{m} \cdot \mathbf{B}_i^*]$  has been extensively employed for characterizing dipole optical interactions [27–29]. We thus expect that progress on research of radiation-matter interactions with chiral fields will give rise to a growing use of the helicity extinction in Eq. (1.2):  $(2\pi c/\mu) \Re\{-\epsilon^{-1} \mathbf{p} \cdot \mathbf{B}_i^* + \mu \mathbf{m} \cdot \mathbf{E}_i^*\}$ . Based on this reasoning we find it natural to introduce an *enhancement factor*  $F_{\mathcal{H}}$  for the emission of helicity in analogy with the Purcell factor for a radiating electric and/or magnetic dipole:  $F = 1 + (3/2k^3) \Im[\mathbf{p} \cdot \mathbf{E}_i^* + \mathbf{m} \cdot \mathbf{B}_i^*] / [\epsilon^{-1} |\mathbf{p}|^2 + \mu |\mathbf{m}|^2]$ , viz. :

$$F_{\mathcal{H}} = 1 + \frac{3\epsilon}{4\mu k^3} \frac{\Re\{-\frac{1}{\epsilon} \mathbf{p} \cdot \mathbf{B}_i^* + \mu \mathbf{m} \cdot \mathbf{E}_i^*\}}{\Im[\mathbf{p} \cdot \mathbf{m}^*]}. \quad (1.4)$$

In this connection, and analogously to the complex Poynting vector theorem of energy conservation, (see Sec 6.10 of [30] and also [21]), the integration of the above mentioned continuity equation for a lossy particle of volume  $V$  with constitutive parameters  $\epsilon = \epsilon_R + i\epsilon_I$  and  $\mu = \mu_R + i\mu_I$

$i\mu_I$ , in absence of induced currents, yields (1.2) with:  $\mathcal{W}_{\mathcal{H}}^a = \frac{c^2}{2\pi\epsilon} \int_V dv (\epsilon_R \mu_I + \epsilon_I \mu_R) \Im \left\{ \frac{\mathbf{E} \cdot \mathbf{B}^*}{\mu^*} \right\}$ ; which links fields in, or close to, the object with those in any other region of space; in particular in the far-zone.

## 2. The angular spectrum of circularly polarized plane wave components

We address the wide variety of fields propagating in a half-space  $z > 0$ , or  $z < 0$ , free from sources, represented by an angular spectrum of plane waves [31,32]. This includes optical fields. Such representation of either incident and scattered fields, with subindex  $i$  and  $s$  respectively, is:

$$\mathbf{E}_{i,s}(\mathbf{r}) = \int_{\mathcal{D}} \mathbf{e}_{i,s}(\mathbf{s}_{\perp}) e^{ik(\mathbf{s} \cdot \mathbf{r})} d\Omega, \quad \mathbf{B}_{i,s}(\mathbf{r}) = \int_{\mathcal{D}} \mathbf{b}_{i,s}(\mathbf{s}_{\perp}) e^{ik(\mathbf{s} \cdot \mathbf{r})} d\Omega. \quad (2.1)$$

The integration being done on the contour  $\mathcal{D}$  that contains both propagating and evanescent waves [31,32].  $\mathbf{s} = (\mathbf{s}_{\perp}, s_z)$  is the unit wavevector of the plane wave component of amplitude  $\mathbf{e}_{i,s}(\mathbf{s}_{\perp})$  and  $\mathbf{b}_{i,s}(\mathbf{s}_{\perp})$ , where  $\mathbf{s}_{\perp} = (s_x, s_y, 0)$  and  $s_z = \pm \sqrt{1 - |\mathbf{s}_{\perp}|^2}$  if  $|\mathbf{s}_{\perp}|^2 \leq 1$ , (propagating components); and  $s_z = \pm i\sqrt{|\mathbf{s}_{\perp}|^2 - 1}$  if  $|\mathbf{s}_{\perp}|^2 > 1$ , (evanescent components).  $d\Omega = \sin \alpha d\alpha d\beta$ .  $s_x = \sin \alpha \cos \beta$ ,  $s_y = \sin \alpha \sin \beta$ ,  $s_z = \cos \alpha$ .  $0 \leq \beta \leq 2\pi$ ,  $0 \leq \alpha \leq \pi/2$  for propagating components and  $\alpha = \pi/2 - i\delta$ ,  $0 < \delta \leq \infty$  for evanescent components. The + or – sign in  $s_z$  applies according to whether propagation is in  $z > 0$  or  $z < 0$ , respectively. We shall assume the first case. For  $z < 0$  the results are similar. In general all plane wave components are elliptically polarized. For the

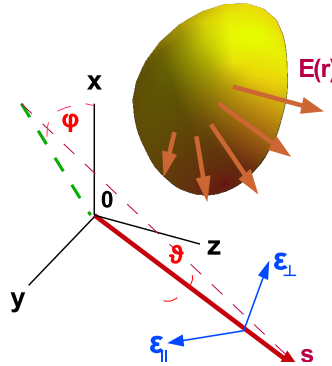


**Figure 1.** (Color online). A field  $\mathbf{E}(\mathbf{r})$ , with wavefront shown by the brown-yellow surface, propagates into the half-space  $z > 0$  along arbitrary directions, (light-brown arrows). In the  $OXYZ$  framework the propagation vector along  $\mathbf{s}$  of each plane wave component of  $\mathbf{E}(\mathbf{r})$  has polar and azimuthal angles  $\theta$  and  $\phi$ . The polarization of each of these plane waves is characterized by the orthonormal system  $\{\epsilon_{\perp}, \epsilon_{\parallel}, \mathbf{s}\}$ . The unit vector  $\epsilon_{\parallel}$  is in the polar plane containing both  $\mathbf{s}$  and its projection (green broken line) on  $OXY$ , and points in the rotation sense of  $\theta$ . On the other hand,  $\epsilon_{\perp}$  is normal to this plane and points against the sense of rotation of  $\phi$ .

incident and scattered fields one has:  $\mathbf{b}_{i,s}(\mathbf{s}_{\perp}) = n\mathbf{s} \times \mathbf{e}_{i,s}(\mathbf{s}_{\perp})$ ,  $\mathbf{e}_{i,s}(\mathbf{s}_{\perp}) \cdot \mathbf{s} = \mathbf{b}_{i,s}(\mathbf{s}_{\perp}) \cdot \mathbf{s} = 0$ . The complex amplitudes of the scattered, or radiated, field angular spectrum being:

$$\mathbf{e}_s(\mathbf{s}_{\perp}) = k^2 [\epsilon^{-1}(\mathbf{s} \times \mathbf{p}) \times \mathbf{s} - \sqrt{\frac{\mu}{\epsilon}}(\mathbf{s} \times \mathbf{m})]; \quad \mathbf{b}_s(\mathbf{s}_{\perp}) = k^2 [\mu(\mathbf{s} \times \mathbf{m}) \times \mathbf{s} + \sqrt{\frac{\mu}{\epsilon}}(\mathbf{s} \times \mathbf{p})]. \quad (2.2)$$

For each plane wave component with wavevector  $k\mathbf{s}$  of either the incident or the scattered field (2.1), we consider an orthonormal set of unit vectors (cf. Fig. 1)  $\{\hat{\epsilon}_{\perp}, \hat{\epsilon}_{\parallel}, \mathbf{s}\}$  from which we define an helicity basis of rotating vectors:  $\epsilon^{\pm}(\mathbf{s}) = (1/\sqrt{2})(\hat{\epsilon}_{\perp}(\mathbf{s}) \pm i\hat{\epsilon}_{\parallel}(\mathbf{s}))$ ,  $\epsilon^{\pm*}(\mathbf{s}) \cdot \epsilon^{\mp}(\mathbf{s}) = 0$ . Then

each incident or scattered component complex amplitude is expressed as the sum of a left-handed (LCP, sign "+") and a right-handed (RCP, sign "-") circularly polarized plane wave in its corresponding framework  $\{\hat{\mathbf{e}}_{\perp}, \hat{\mathbf{e}}_{\parallel}, \mathbf{s}\}$  according to

$$\mathbf{e}_{i,s}(\mathbf{s}_{\perp}) = e_{i,s}^{+}(\mathbf{s}_{\perp})\boldsymbol{\epsilon}^{+}(\mathbf{s}) + e_{i,s}^{-}(\mathbf{s}_{\perp})\boldsymbol{\epsilon}^{-}(\mathbf{s}). \quad (2.3)$$

$$\mathbf{b}_{i,s}(\mathbf{s}_{\perp}) = b_{i,s}^{+}(\mathbf{s}_{\perp})\boldsymbol{\epsilon}^{+}(\mathbf{s}) + b_{i,s}^{-}(\mathbf{s}_{\perp})\boldsymbol{\epsilon}^{-}(\mathbf{s}) = -ni[e_{i,s}^{+}(\mathbf{s}_{\perp})\boldsymbol{\epsilon}^{+}(\mathbf{s}) - e_{i,s}^{-}(\mathbf{s}_{\perp})\boldsymbol{\epsilon}^{-}(\mathbf{s})]. \quad (2.4)$$

With equation  $\nabla \cdot \mathbf{E} = 0$  imposing according to (2.1) that  $\boldsymbol{\epsilon}^{\pm}(\mathbf{s}) \cdot \mathbf{s} = 0$ . In this representation, the helicity density of each incident or scattered plane wave component reads:

$$\mathcal{H}^{i,s}(\mathbf{s}_{\perp}) = (\epsilon/k)\Im[e_{i,sx}^{*}(\mathbf{s}_{\perp})e_{i,sy}(\mathbf{s}_{\perp})] = (\epsilon/2k)S_3(\mathbf{s}_{\perp}) = (\epsilon/2k)[|e_{i,s}^{+}(\mathbf{s}_{\perp})|^2 - |e_{i,s}^{-}(\mathbf{s}_{\perp})|^2]. \quad (2.5)$$

I.e. as the difference between the LCP and RCP intensities of this angular component of wavevector  $k\mathbf{s}$ .  $S_3(\mathbf{s}_{\perp})$  is the 4th Stokes parameter [26,33]. Also  $|e_{i,s}(\mathbf{s}_{\perp})|^2 = |e_{i,sx}(\mathbf{s}_{\perp})|^2 + |e_{i,sy}(\mathbf{s}_{\perp})|^2 = \frac{8\pi}{c}\sqrt{\frac{\mu}{\epsilon}} < S_{i,s}(\mathbf{s}_{\perp}) > = \frac{8\pi}{\epsilon} < w_{i,s}(\mathbf{s}_{\perp}) > \cdot < S_{i,s}(\mathbf{s}_{\perp}) >$  and  $< w_{i,s}(\mathbf{s}_{\perp}) >$  representing the time-averaged Poynting vector magnitude and electromagnetic energy density, respectively:

$$< w_{i,s}(\mathbf{s}_{\perp}) > = < w_{e,i,s}(\mathbf{s}_{\perp}) > + < w_{m,i,s}(\mathbf{s}_{\perp}) > \cdot < w_{e,i,s}(\mathbf{s}_{\perp}) > = (\epsilon/16\pi)|\mathbf{e}_{i,s}(\mathbf{s}_{\perp})|^2, < w_{m,i,s}(\mathbf{s}_{\perp}) > = (1/16\pi\mu)|\mathbf{b}_{i,s}(\mathbf{s}_{\perp})|^2.$$

Therefore for the incident or the scattered field we have from (2.1), (2.3) and (2.4) the following splitting into LCP and RCP waves

$$\mathbf{E}_{i,s}(\mathbf{r}) = \mathbf{E}_{i,s}^{+}(\mathbf{r}) + \mathbf{E}_{i,s}^{-}(\mathbf{r}); \quad \mathbf{B}_{i,s}(\mathbf{r}) = \mathbf{B}_{i,s}^{+}(\mathbf{r}) + \mathbf{B}_{i,s}^{-}(\mathbf{r}) = -ni[\mathbf{E}_{i,s}^{+}(\mathbf{r}) - \mathbf{E}_{i,s}^{-}(\mathbf{r})]. \quad (2.6)$$

$$\mathbf{E}_{i,s}^{\pm}(\mathbf{r}) = \int_{\mathcal{D}} e_{i,s}^{\pm}(\mathbf{s}_{\perp})\boldsymbol{\epsilon}^{\pm}(\mathbf{s})e^{ik(\mathbf{s} \cdot \mathbf{r})}d\Omega. \quad (2.7)$$

Assuming the particle chiral,  $\alpha_{em} = -\alpha_{me}$ , and introducing Eqs.(2.7) into (1.1) we write:

$$\mathbf{p}(\mathbf{r}) = \mathbf{p}_{+}(\mathbf{r}) + \mathbf{p}_{-}(\mathbf{r}); \quad \mathbf{m}(\mathbf{r}) = \mathbf{m}_{+}(\mathbf{r}) + \mathbf{m}_{-}(\mathbf{r}). \quad (2.8)$$

With

$$\mathbf{p}_{\pm}(\mathbf{r}) = (\alpha_e \pm ni\alpha_{me})\mathbf{E}_i^{\pm}(\mathbf{r}). \quad \mathbf{m}_{\pm}(\mathbf{r}) = (\alpha_{me} \mp ni\alpha_m)\mathbf{E}_i^{\pm}(\mathbf{r}). \quad (2.9)$$

And substituting (2.1) into (2.9) we see that  $\mathbf{p}_{\pm}(\mathbf{r})$  and  $\mathbf{m}_{\pm}(\mathbf{r})$  also admit an angular spectrum representation like (2.1), their respective angular spectra being:

$$\hat{\mathbf{p}}_{\pm}(\mathbf{s}_{\perp}) = (\alpha_e \pm ni\alpha_{me})e_i^{\pm}(\mathbf{s}_{\perp})\boldsymbol{\epsilon}^{\pm}(\mathbf{s}); \quad \hat{\mathbf{m}}_{\pm}(\mathbf{s}_{\perp}) = (\alpha_{me} \mp ni\alpha_m)e_i^{\pm}(\mathbf{s}_{\perp})\boldsymbol{\epsilon}^{\pm}(\mathbf{s}). \quad (2.10)$$

So that from (2.10), (2.8) and (2.2) we obtain for the scattered field angular spectrum:

$$\begin{aligned} e_s^{\pm}(\mathbf{s}_{\perp}) &= k^2 \left[ \frac{\alpha_e \pm ni\alpha_{me}}{\epsilon} \pm i\sqrt{\frac{\mu}{\epsilon}}(\alpha_{me} \mp ni\alpha_m) \right] e_i^{\pm}(\mathbf{s}_{\perp}). \\ b_s^{\pm}(\mathbf{s}_{\perp}) &= k^2 [\mp i\sqrt{\frac{\mu}{\epsilon}}(\alpha_e \pm ni\alpha_{me}) + \mu(\alpha_{me} \mp ni\alpha_m)] e_i^{\pm}(\mathbf{s}_{\perp}). \end{aligned} \quad (2.11)$$

We obtain the helicity densities  $\mathcal{H}_{i,s}$  for either the incident or scattered fields by introducing (2.3) and (2.4) into (2.1), and inserting the result into the definition introduced in Section 1(a):  $\mathcal{H} = < \mathcal{H} > = \frac{1}{2k}\sqrt{\frac{\epsilon}{\mu}}\Im(\mathbf{E} \cdot \mathbf{B}^*)$ . Then since after taking imaginary parts the cross-terms containing the integrand factors  $nie_{i,s}^{+}(\mathbf{s}_{\perp})e_{i,s}^{-*}(\mathbf{s}'_{\perp})\boldsymbol{\epsilon}^{+}(\mathbf{s}) \cdot \boldsymbol{\epsilon}^{-*}(\mathbf{s}')$  and  $-nie_{i,s}^{+*}(\mathbf{s}_{\perp})e_{i,s}^{-}(\mathbf{s}'_{\perp})\boldsymbol{\epsilon}^{+*}(\mathbf{s}) \cdot \boldsymbol{\epsilon}^{-}(\mathbf{s}')$  cancel each other, we finally get:

$$\mathcal{H}_{i,s}(\mathbf{r}) = \frac{\epsilon}{2k}[|\mathbf{E}_{i,s}^{+}(\mathbf{r})|^2 - |\mathbf{E}_{i,s}^{-}(\mathbf{r})|^2]. \quad (2.12)$$

Equation (2.12) introduced in the optical theorem for the helicity, (1.2), accounts for all chirality effects due to the interaction of waves with dipolar particles, both in the propagating region (real  $s_i^z$ ) of the angular spectrum, as in the evanescent domain (imaginary  $s_i^z$ ). The latter applies in particular for the interaction of plasmon polaritons with particles on metallic surfaces.

Expressions (2.12) are of particular importance in the far zone  $kr \rightarrow \infty$ , where [31,32]

$$\mathbf{E}_{i,s}^{\pm}(r\hat{\mathbf{s}}) \approx -(2\pi i/k)e_{i,s}^{\pm}(\hat{\mathbf{s}}_{\perp})\boldsymbol{\epsilon}^{\pm}(\hat{\mathbf{s}})\exp(ikr)/r. \quad (2.13)$$

$e_s^{\pm}(\hat{\mathbf{s}}_{\perp})\boldsymbol{\epsilon}^{\pm}(\hat{\mathbf{s}})$  playing the role of the CPL complex amplitude for a radiated, or scattered, field, and  $\hat{\mathbf{s}} = \mathbf{r}/r$  now belonging to the domain of propagating components only. Dropping the subindices  $i, s$  to simplify notation, Eqs.(2.12) and (2.13) lead for either the incident or the scattered field to:

$$\mathcal{H}_{ff}(r\hat{\mathbf{s}}) = \frac{2\pi^2\epsilon}{k^3r^2} [|e^{+}(\hat{\mathbf{s}}_{\perp})|^2 - |e^{-}(\hat{\mathbf{s}}_{\perp})|^2]. \quad (2.14)$$

And their density of flow of helicity is:  $\mathcal{F}_{ff}(r\hat{\mathbf{s}}) = \frac{c}{n}\mathcal{H}_{ff}(\mathbf{r})\hat{\mathbf{s}}$ ; which in agreement with the conservation of helicity, expresses on integration in a large sphere surrounding the scatterer that the outgoing helicity flow of the field across any plane  $z = \text{constant}$ , or closed surface, outside the scattering volume, which equals the flow of helicity across any sphere at infinity, is equal to  $c/n$  times the total helicity enclosed by that sphere:  $\int \int_{z=0} \mathcal{F}(\mathbf{r}) \cdot \hat{\mathbf{z}} dx dy = \int_{r \rightarrow \infty} \mathcal{F}_{ff}(r\hat{\mathbf{s}}) \cdot \mathbf{r} r^2 d\Omega$ . Where now the solid angle  $\Omega$  spans on the whole sphere of real angles only. Taking into account (2.12), and in analogy with the flow of energy [31,32], one sees that the evanescent components do not contribute to the flux of helicity across the plane  $z = 0$  in the half-space  $z \geq 0$ .

### (a) A particular case: Incident elliptically polarized plane wave

The significance of the optical theorem (1.2) for the helicity - or chirality - of wavefields is illustrated considering one of the simplest and most employed configurations: one elliptically polarized incident plane wave impinging on a dipolar particle with wavevector  $k\mathbf{s}_i$  along  $OZ$ . According to (2.3) and (2.4) the fields are:

$$\begin{aligned} \mathbf{e}_i &= (e_{ix}, e_{iy}, 0) = e_i^{+}\boldsymbol{\epsilon}^{+} + e_i^{-}\boldsymbol{\epsilon}^{-}. \\ \mathbf{b}_i &= (b_{ix}, b_{iy}, 0) = n(-e_{iy}, e_{ix}, 0) = b_i^{+}\boldsymbol{\epsilon}^{+} + b_i^{-}\boldsymbol{\epsilon}^{-} = -ni(e_i^{+}\boldsymbol{\epsilon}^{+} - e_i^{-}\boldsymbol{\epsilon}^{-}). \end{aligned}$$

So that the incident helicity density reads:

$$\mathcal{H}^i = (\epsilon/k)\Im[e_{ix}^{*}e_{iy}] = (\epsilon/2k)S_3 = (\epsilon/2k)[|e_i^{+}|^2 - |e_i^{-}|^2]. \quad (2.15)$$

Also, according to (2.8) and (2.9):

$$\mathbf{p} = p_{+}\boldsymbol{\epsilon}^{+} + p_{-}\boldsymbol{\epsilon}^{-}, \quad p_{\pm} = (\alpha_e \mp ni\alpha_{em})e_i^{\pm}; \quad \mathbf{m} = m_{+}\boldsymbol{\epsilon}^{+} + m_{-}\boldsymbol{\epsilon}^{-}, \quad m_{\pm} = (\alpha_{me} \mp ni\alpha_m)e_i^{\pm}.$$

On introducing these dipole moments and fields into the optical theorems of helicity (1.2) and energy (1.3), they yield for the rate of helicity and energy extinction:

$$\Im\{(p_{+} + inm_{+})e_i^{+*} - (p_{-} - inm_{-})e_i^{-*}\} = \frac{4k^3n}{3\epsilon}\Im\{p_{+}m_{+}^{*} + p_{-}m_{-}^{*}\} + \mathcal{W}_{\mathcal{H}}^a \quad (2.16)$$

and

$$\Im\{(p_{+} + inm_{+})e_i^{+*} + (p_{-} - inm_{-})e_i^{-*}\} = \frac{2k^3}{3\epsilon}\{|p_{+}|^2 + |p_{-}|^2 + n^2(|m_{+}|^2 + |m_{-}|^2)\} + \mathcal{W}^a, \quad (2.17)$$

respectively. Eq. (2.16) is identical to the CD law, usually mechanoquantically formulating molecular absorption and fluorescence effects [18]. However Eqs. (2.16) and (2.17), obtained from classical electrodynamics, include the rate of helicity and energy dissipation both by absorption and scattering (or diffraction), and generalize the CD theory to any wide sense dipolar "particle" or structure.

In other words, the CD phenomenon is not only characterized by the operation of taking the difference of energy absorption and emission  $\Im[\mathbf{p} \cdot \mathbf{E}_i^{*} + \mathbf{m} \cdot \mathbf{B}_i^{*}]$  by chiral molecules as they are separately illuminated by RCP and LCP waves; i.e as this absorbed energy is  $\Im\{(p_{+} + inm_{+})e_i^{+*}\}$  and  $\Im\{(p_{-} - inm_{-})e_i^{-*}\}$ , respectively, as usually considered so far [17–19]. But CD is also, and fundamentally, one of the physical manifestations of the conservation law of electromagnetic helicity -or chirality- and is represented by the left-side term of (2.16),  $\Re[-\frac{1}{\epsilon}\mathbf{p} \cdot \mathbf{B}_i^{*} + \mu\mathbf{m} \cdot \mathbf{E}_i^{*}] = \Im\{(p_{+} + inm_{+})e_i^{+*} - (p_{-} - inm_{-})e_i^{-*}\}$  of the helicity optical theorem (1.2); being involved in any scattering and/or absorption process of LCP and RCP electromagnetic waves, thus characterizing the rate of extinction of helicity - or chirality-. In addition, as shown by Eqs. (2.10) and (2.16), CD arises not only due the chirality of the



scattering object, represented by  $\alpha_{me}$ , but also and primarily by the mere induction of their electric and/or magnetic dipoles, whose responses are characterized by  $\alpha_e$  and  $\alpha_m$ , respectively.

Hence it is not surprising that the ratio of the extinction of incident field helicity (2.16) and energy (2.17) is identical to the well-known *dissymmetry factor* of CD [4,17,19]. Moreover, adding and subtracting (2.16) and (2.17) yield the energy excitation by extinction of the respective LCP or RCP component of the incident elliptically polarized light according to the dipole handedness  $p_{\pm}$  and/or  $m_{\pm}$ :

$$\Im\{(p_{\pm} \pm inm_{\pm})e_i^{\pm*}\} = \frac{k^3}{3\epsilon}\{|p_{+} \pm inm_{+}|^2 + |p_{-} \pm inm_{-}|^2\} + \frac{1}{2}(\mathcal{W}^a \pm \mathcal{W}_{\mathcal{H}}^a). \quad (2.18)$$

## (b) The special case of an incident circularly polarized plane wave

Let the field incident on the particle be just one CPL component, either LCP or RCP, then  $e_i^{\pm} = e\epsilon^{\pm}$  and  $\mathbf{p} = p_{\pm}\epsilon^{\pm}$ ,  $\mathbf{m} = m_{\pm}\epsilon^{\pm}$ , and (2.18) lead to

$$\Im\{(p_{\pm} \pm inm_{\pm})e_i^{\pm*}\} = \frac{k^3}{3\epsilon}\{|p_{\pm}|^2 + n^2|m_{\pm}|^2 \pm 2n\Im\{p_{\pm}m_{\pm}^*\}\} + \frac{1}{2}(\mathcal{W}^a \pm \mathcal{W}_{\mathcal{H}}^a). \quad (2.19)$$

and

$$\frac{k^3}{3\epsilon}|p_{\pm} \mp inm_{\pm}|^2 + \frac{1}{2}(\mathcal{W}^a \mp \mathcal{W}_{\mathcal{H}}^a) = 0. \quad (2.20)$$

From which we obtain

$$2n\Im\{p_{\pm}m_{\pm}^*\} = \pm[|p_{\pm}|^2 + n^2|m_{\pm}|^2 + \frac{1}{2}(\mathcal{W}^a \mp \mathcal{W}_{\mathcal{H}}^a)]. \quad (2.21)$$

Thus, apart from a constant factor, for CPL incidence the scattered helicity equals in modulus the scattered energy plus the rates of dissipation of helicity and energy, and has a sign that depends on the handedness of the incident light. Of course (2.19) - (2.21) are consistent, as they should, with Eqs.(2.16) and (2.17), which for CPL become:

$$\Im\{(p_{\pm} \pm inm_{\pm})e_i^{\pm*}\} = \pm \frac{4k^3n}{3\epsilon}\Im\{p_{\pm}m_{\pm}^*\} \pm \mathcal{W}_{\mathcal{H}}^a = \frac{2k^3}{3\epsilon}\{|p_{\pm}|^2 + n^2|m_{\pm}|^2\} + \mathcal{W}^a. \quad (2.22)$$

A Comparison of (2.22) with (2.16) and (2.17), shows that the excitation of the particle by both the LCP and RCP components of an elliptically polarized plane wave, is equivalent to performing two observations separately: one with an LCP plane wave only, and another one with only RCP, (each of which is ruled by (2.22) with the corresponding sign), and then subtracting or adding the respective excitations given by the left sides of (2.22). This operation reproduces the left side of (2.16) and (2.17), respectively. In other words, Eqs.(2.16) and (2.17) show that *the LCP and RCP components of an incident elliptically polarized plane wave do not interfere and, hence, interact independently of each other with the particle.*

As regards Eq. (2.20), since often in molecular spectroscopy  $|m_{\pm}| \ll |p_{\pm}|$ , the value of  $\mathcal{W}^a$  and/or  $\mathcal{W}_{\mathcal{H}}^a$  contributes to that of  $|p_{\pm}|$ . Nonetheless Eq. (2.20) is also compatible with the electric and magnetic dipoles excited by CPL light, and the absorption rates, fulfilling:

$$p_{\pm} = \pm inm_{\pm} \Leftrightarrow \mathcal{W}_{\mathcal{H}}^a = \pm \mathcal{W}^a. \quad (2.23)$$

Hence *this is a sufficient condition for an electric-magnetic dipole to emit chiral light*. Particularly remarkable is this latter case is when the dissipation rates of helicity and energy either cancel each other, or the particle introduces no energy nor helicity losses,  $\mathcal{W}^a = \mathcal{W}_{\mathcal{H}}^a = 0$ , so that all energy and helicity extinguished from the incident field are re-radiated by elastic scattering. As seen from (2.20), in that case:  $2n\Im\{p_{\pm}m_{\pm}^*\} = \pm[|p_{\pm}|^2 + n^2|m_{\pm}|^2]$ , which states that then the optical theorems for helicity, Eq. (2.16), and energy, Eq. (2.17), are equivalent, and the scattered helicity is proportional to the scattered intensity and has a sign that depends on the handedness of the incident light, whereas the density of helicity flow (spin) is proportional to that of energy flow (Poynting vector). Thus in such a situation the optical theorems for helicity (1.2) and energy (1.3) are equivalent, (see also [6,16]).

Equation (2.23) also has some important consequences:

- *The far-zone scattered field is circularly polarized.*  $\mathbf{b}^\pm(\mathbf{s}_\perp) = \mp n i e^\pm(\mathbf{s}_\perp)$ , [cf. Eqs. (2.2)]. This circular polarization holds with respect to the Cartesian system of orthogonal axes defined by the unit vectors:  $(\epsilon_\perp, \epsilon_\parallel, \mathbf{s})$ , (see Fig. 1).  $\epsilon_\perp$  and  $\epsilon_\parallel$  being respectively perpendicular and parallel to the polar plane (which now becomes the scattering plane) delimited by  $\mathbf{s}$  and its projection on  $OXY$ . I.e.:  $\mathbf{e}^\pm(\mathbf{s}_\perp) = (\mathbf{e}(\mathbf{s}_\perp) \cdot \epsilon_\perp)(\epsilon_\perp + \pm i\epsilon_\parallel + 0\mathbf{s})$  and  $\mathbf{b}^\pm(\mathbf{s}_\perp) = (n\mathbf{e}(\mathbf{s}_\perp) \cdot \epsilon_\perp)(\mp i\epsilon_\perp + \epsilon_\parallel + 0\mathbf{s})$ .

From the above it should also be noticed that *it is the handedness of the dipole moments, and not necessarily the chirality  $\alpha_{me}$ , the relevant characteristic for these CD effects*. Besides, this CPL property of the scattered field is just a consequence of the optical theorems of energy and helicity, and does not presuppose in the particle neither chirality,  $\alpha_{em} = -\alpha_{me}$ , nor duality,  $\epsilon^{-1}\alpha_e = \mu\alpha_m$  [16]. Although the combination of both theorems imposes [16] that the existence of one these two latter properties of the particle polarizabilities implies the other.

- *In the near field zone, the scattered wave in the basis  $(\epsilon_\perp, \epsilon_\parallel, \mathbf{s})$  has*

$$\begin{aligned}\mathbf{E}_{nf}(\mathbf{r}) &= \frac{1}{\epsilon r^3} [3\mathbf{s}(\mathbf{s} \cdot \mathbf{p}) - \mathbf{p}] = -\frac{p_\pm}{\epsilon r^3} e^{\pm i\phi} [\pm i\epsilon_\perp + \cos\theta \epsilon_\parallel - 2\sin\theta \mathbf{s}]. \\ \mathbf{B}_{nf}(\mathbf{r}) &= \frac{\mu}{r^3} [3\mathbf{s}(\mathbf{s} \cdot \mathbf{m}) - \mathbf{m}] = -\frac{\mu m_\pm}{r^3} e^{\pm i\phi} [\pm i\epsilon_\perp + \cos\theta \epsilon_\parallel - 2\sin\theta \mathbf{s}].\end{aligned}\quad (2.24)$$

Thus this field *being CPL* at points  $\mathbf{r}$  along the polar axis  $OZ$ , ( $\theta = 0$ , or  $\theta = \pi$ ).

### 3. Excitation of helicity and energy with general optical fields: The role of angular spectra with right circular and left circular polarization

Returning to Eqs. (2.6)-(2.10) for general optical fields, we have from the optical theorem for the helicity (1.2) the following expression for its extinction from the incident field on scattering by the particle induced dipole:

$$\begin{aligned}& \Im\{[\mathbf{p}_+(\mathbf{r}) + in\mathbf{m}_+(\mathbf{r})] \cdot \mathbf{E}_i^{+*}(\mathbf{r}) - [\mathbf{p}_-(\mathbf{r}) - in\mathbf{m}_-(\mathbf{r})] \cdot \mathbf{E}_i^{-*}(\mathbf{r})\} + 2\Re\{\alpha_e - n^2\alpha_m\} \\ & \times \Im\{\mathbf{E}_i^-(\mathbf{r}) \cdot \mathbf{E}_i^{+*}(\mathbf{r})\} = \frac{4k^3 n}{3\epsilon} \Im\{[\mathbf{p}_+(\mathbf{r}) \cdot \mathbf{m}_+^*(\mathbf{r}) + \mathbf{p}_-(\mathbf{r}) \cdot \mathbf{m}_-^*(\mathbf{r})] + CD(\mathbf{r}) + \frac{n}{2\pi c} \mathcal{W}_{\mathcal{J}\mathcal{E}}^a\}.\end{aligned}\quad (3.1)$$

While the extinction of incident energy is according to the standard optical theorem (1.3):

$$\begin{aligned}& \Im\{[\mathbf{p}_+(\mathbf{r}) + in\mathbf{m}_+(\mathbf{r})] \cdot \mathbf{E}_i^{+*}(\mathbf{r}) + [\mathbf{p}_-(\mathbf{r}) - in\mathbf{m}_-(\mathbf{r})] \cdot \mathbf{E}_i^{-*}(\mathbf{r})\} + 2\Im\{\alpha_e - n^2\alpha_m\} \\ & \times \Re\{\mathbf{E}_i^-(\mathbf{r}) \cdot \mathbf{E}_i^{+*}(\mathbf{r})\} = \frac{2k^3}{3\epsilon} \{|\mathbf{p}_+(\mathbf{r})|^2 + |\mathbf{p}_-(\mathbf{r})|^2 + n^2[|\mathbf{m}_+(\mathbf{r})|^2 + |\mathbf{m}_-(\mathbf{r})|^2]\} + CE(\mathbf{r}) + \frac{2}{\omega} \mathcal{W}^a.\end{aligned}\quad (3.2)$$

The terms  $CD(\mathbf{r})$  and  $CE(\mathbf{r})$  are

$$CD(\mathbf{r}) = \frac{8k^3 n}{3\epsilon} [\Im\{(\alpha_e - n^2\alpha_m)\alpha_{me}^*\} \Re\{\mathbf{E}_i^-(\mathbf{r}) \cdot \mathbf{E}_i^{+*}(\mathbf{r})\} - n \Im\{\alpha_e \alpha_m^*\} \Im\{\mathbf{E}_i^-(\mathbf{r}) \cdot \mathbf{E}_i^{+*}(\mathbf{r})\}]. \quad (3.3)$$

$$\begin{aligned}CE(\mathbf{r}) &= \frac{4k^3}{3\epsilon} \{[|\alpha_e|^2 - n^4|\alpha_m|^2] \Re\{\mathbf{E}_i^-(\mathbf{r}) \cdot \mathbf{E}_i^{+*}(\mathbf{r})\} \\ & + 2n \Re\{(\alpha_e - n^2\alpha_m)\alpha_{me}^*\} \Im\{\mathbf{E}_i^-(\mathbf{r}) \cdot \mathbf{E}_i^{+*}(\mathbf{r})\}.\end{aligned}\quad (3.4)$$

In these equations  $\mathbf{r}$  denotes the position vector of the center of the particle immersed in the illuminating field. Now, in contrast with the scattering of an incident elliptically polarized plane wave discussed above, the scattered helicity and energy convey interference between  $\mathbf{E}_i^-$  and  $\mathbf{E}_i^+$ .

Notice that by virtue of the asymptotic expression (2.13), in the far-zone  $CD(r\hat{\mathbf{s}}) = CE(r\hat{\mathbf{s}}) = 0$  since  $\epsilon^\pm(\hat{\mathbf{s}}) \cdot \epsilon^\mp(\hat{\mathbf{s}}) = 0$ . It is also interesting to observe from (3.1)-(3.4) that if the particle is dual,  $\alpha_e = n^2\alpha_m$ , the terms of interference between  $\mathbf{E}^+$  and  $\mathbf{E}^-$  are zero and so are  $CD(\mathbf{r})$  and  $CE(\mathbf{r})$  for any  $\mathbf{r}$ . Then (3.1) and (3.2) reduce to equations similar to (2.16) and (2.17).



However the important point is that now the appearance of the interference factor  $[\mathbf{E}_i^-(\mathbf{r}) \cdot \mathbf{E}_i^{+*}(\mathbf{r})]$  in (3.1) and (3.2) allows one to choose the incident field such that either  $\Im[\mathbf{E}_i^- \cdot \mathbf{E}_i^{+*}]$  or  $\Re[\mathbf{E}_i^- \cdot \mathbf{E}_i^{+*}]$  is zero, or small, for the helicity extinction (3.1) and for the intensity extinction (3.2), respectively. We thus shall analyse the consequences of  $2\Re\{\alpha_e - n^2\alpha_m\}\Im\{\mathbf{E}_i^- \cdot \mathbf{E}_i^{+*}\}$  or  $2\Im\{\alpha_e - n^2\alpha_m\}\Re\{\mathbf{E}_i^- \cdot \mathbf{E}_i^{+*}\}$  being non-zero in the left sides of (3.1) and (3.2), respectively, as a consequence of the choice of illumination on the particle.

Using (2.9) the left sides of (3.1) and (3.2) are in terms of the polarizabilities and fields:

$$\begin{aligned} & \Im\{[\mathbf{p}_+(\mathbf{r}) + in\mathbf{m}_+(\mathbf{r})] \cdot \mathbf{E}_i^{+*}(\mathbf{r}) \pm [\mathbf{p}_-(\mathbf{r}) - in\mathbf{m}_-(\mathbf{r})] \cdot \mathbf{E}_i^{-*}(\mathbf{r})\} = \\ & \Im\{\alpha_e + n^2\alpha_m\}(|\mathbf{E}_i^+(\mathbf{r})|^2 \mp |\mathbf{E}_i^-(\mathbf{r})|^2) + 2n\Re\{\alpha_{me}\}(|\mathbf{E}_i^+(\mathbf{r})|^2 \pm |\mathbf{E}_i^-(\mathbf{r})|^2). \end{aligned} \quad (3.5)$$

Using (3.5) we now address the rate of extinction of helicity  $\mathcal{W}_{\mathcal{H}}^s$  (cf. Eq. (17) in [16]) and energy  $\mathcal{W}^s$  in the particle, given by the left sides of (3.1) and (3.2), as functions of the polarizabilities:

$$\begin{aligned} \frac{\mu}{2\pi c} \mathcal{W}_{\mathcal{H}}^s & \equiv \Im\{[\mathbf{p}_+(\mathbf{r}) + in\mathbf{m}_+(\mathbf{r})] \cdot \mathbf{E}_i^{+*}(\mathbf{r}) - [\mathbf{p}_-(\mathbf{r}) - in\mathbf{m}_-(\mathbf{r})] \cdot \mathbf{E}_i^{-*}(\mathbf{r})\} \\ & + 2\Re\{\alpha_e - n^2\alpha_m\}\Im\{\mathbf{E}_i^-(\mathbf{r}) \cdot \mathbf{E}_i^{+*}(\mathbf{r})\} = \{\Im\{\alpha_e + n^2\alpha_m\}(|\mathbf{E}_i^+(\mathbf{r})|^2 - |\mathbf{E}_i^-(\mathbf{r})|^2) \\ & + 2n\Re\{\alpha_{me}\}(|\mathbf{E}_i^+(\mathbf{r})|^2 + |\mathbf{E}_i^-(\mathbf{r})|^2) + 2\Re\{\alpha_e - n^2\alpha_m\}\Im\{\mathbf{E}_i^-(\mathbf{r}) \cdot \mathbf{E}_i^{+*}(\mathbf{r})\}. \end{aligned} \quad (3.6)$$

And

$$\begin{aligned} \frac{2}{\omega} \mathcal{W}^s & \equiv \Im\{[\mathbf{p}_+(\mathbf{r}) + in\mathbf{m}_+(\mathbf{r})] \cdot \mathbf{E}_i^{+*}(\mathbf{r}) + [\mathbf{p}_-(\mathbf{r}) - in\mathbf{m}_-(\mathbf{r})] \cdot \mathbf{E}_i^{-*}(\mathbf{r})\} \\ & + 2\Im\{\alpha_e - n^2\alpha_m\}\Re\{\mathbf{E}_i^-(\mathbf{r}) \cdot \mathbf{E}_i^{+*}(\mathbf{r})\} = \{\Im\{\alpha_e + n^2\alpha_m\}(|\mathbf{E}_i^+(\mathbf{r})|^2 + |\mathbf{E}_i^-(\mathbf{r})|^2) \\ & + 2n\Re\{\alpha_{me}\}(|\mathbf{E}_i^+(\mathbf{r})|^2 - |\mathbf{E}_i^-(\mathbf{r})|^2) + 2\Im\{\alpha_e - n^2\alpha_m\}\Re\{\mathbf{E}_i^-(\mathbf{r}) \cdot \mathbf{E}_i^{+*}(\mathbf{r})\}. \end{aligned} \quad (3.7)$$

Notice that  $\mathcal{W}_{\mathcal{H}}^s \neq 0$  even if  $\alpha_{me} = 0$  and  $|\mathbf{E}_i^+(\mathbf{r})|^2 = |\mathbf{E}_i^-(\mathbf{r})|^2$ . It should be remarked that in the particular case of incident CPL plane waves, or CPL beams without longitudinal component, one has (choosing propagation along e.g.  $OZ$ ):  $\mathbf{E}_i^+ = E_i^+ \boldsymbol{\epsilon}^+$ ,  $\mathbf{E}_i^- = E_i^- \boldsymbol{\epsilon}^-$ ; and since  $\Re\{\mathbf{E}_i^- \cdot \mathbf{E}_i^{+*}\} = \Im\{\mathbf{E}_i^- \cdot \mathbf{E}_i^{+*}\} = 0$ , Eq. (3.1) becomes (2.16) and Eq. (3.2) reduces to (2.17). Hence, in this case  $\mathbf{E}_i^+$  and  $\mathbf{E}_i^-$  do not interfere, and when  $|\mathbf{E}_i^+| = |\mathbf{E}_i^-| = |\mathbf{E}_i|$  Eqs. (3.6) and (3.7) are similar to those of standard circular dichroism which our formulation shows that yields the rate of helicity extinction, first with an incident LCP wave, and then with one being RCP; both of the same amplitude. In such a situation (3.6) and (3.7) become respectively proportional to the well-known numerator:  $4n\alpha_{me}^R |\mathbf{E}_i(\mathbf{r})|^2$  and denominator:  $2(\alpha_e^I + n^2\alpha_m^I) |\mathbf{E}_i(\mathbf{r})|^2$  of the CD *dissymmetry factor* [4,22]. (The superscripts  $R$  and  $I$  denoting real and imaginary part).

However, our general equations (3.6) and (3.7) cover many other configurations, (in particular those so-called superchiral fields [4], which is known, however, to be limited to molecules with  $\alpha_m \simeq 0$  [22]). We next show the broader scope of (3.6) and (3.7) with chiral optical beams possessing a longitudinal component, which as we shall show, plays a key role. We will see that according to whether one chooses such illuminating beams yielding either  $\Re\{\mathbf{E}_i^- \cdot \mathbf{E}_i^{+*}\} = 0$  or  $\Im\{\mathbf{E}_i^- \cdot \mathbf{E}_i^{+*}\} = 0$  one respectively enhances the extinction rate of helicity (3.6) versus that of energy (3.7), (and thus the ratio between them), or viceversa. Notice that since out of resonance the real part of the polarizabilities are usually greater than the imaginary parts, the last term of (3.6) may be larger than that of (3.7). Hence, one may produce bigger enhancement in  $\mathcal{W}_{\mathcal{H}}^s$  than in  $\mathcal{W}^s$  with those choices of  $\Re$  and  $\Im$  of  $\mathbf{E}_i^- \cdot \mathbf{E}_i^{+*}$ .

## 4. Optical beams whose angular spectrum representation contains left circular and right circular plane waves

In the paraxial approximation  $\partial_z \simeq ik_z$ , so that the equation  $\nabla \cdot \mathbf{E} = 0$  implies that  $E_z = (i/k) \nabla_{\perp} \cdot \mathbf{E}_{\perp}$  [34]; ( $\perp$  denotes transversal, i.e.  $XY$  component). The electric vector of an optical

beam is then written in terms of its angular spectrum as [31,32]

$$\mathbf{E}(\mathbf{r}) = e^{ikz} \int_{-\infty}^{\infty} \mathbf{e}(\mathbf{s}_{\perp}) e^{iks_{\perp} \cdot \mathbf{R}} e^{-ikz \frac{|\mathbf{s}_{\perp}|^2}{2}} d^2 \mathbf{s}_{\perp}. \quad (4.1)$$

Having denoted  $\mathbf{r} = (\mathbf{R}, z)$ ,  $\mathbf{R} = (x, y, 0)$ ,  $\mathbf{s} = (\mathbf{s}_{\perp}, s_z)$ ,  $\mathbf{s}_{\perp} = (s_x, s_y, 0)$ .

We shall consider the Gaussian beam; i.e. the one from which other fields, like Hermite and Laguerre-Gaussian beams, are generated [35].

We write for (4.1) the decomposition (2.3) of each component into LCP and RCP waves by expressing the Gaussian angular spectrum [31,32] as

$$\mathbf{e}(\mathbf{s}_{\perp}) = (k^2 W_0^2 / 4\pi) \exp[-k^2 W_0^2 |\mathbf{s}_{\perp}|^2 / 4] [e_0^+ \boldsymbol{\epsilon}^+(\mathbf{s}) + e_0^- \boldsymbol{\epsilon}^-(\mathbf{s})].$$

$e_0^+$  and  $e_0^-$  being complex constants, and  $W_0$  standing for the beam waist at  $z = 0$ . Then we express the beam as:

$$\mathbf{E}(\mathbf{r}) = \frac{(kW_0)^2}{4\pi} e^{ikz} \int_{-\infty}^{\infty} e^{[-k^2 W_0^2 |\mathbf{s}_{\perp}|^2 / 4]} e^{iks_{\perp} \cdot \mathbf{R}} e^{-ikz \frac{|\mathbf{s}_{\perp}|^2}{2}} [e_0^+ \boldsymbol{\epsilon}^+(\mathbf{s}) + e_0^- \boldsymbol{\epsilon}^-(\mathbf{s})] d^2 \mathbf{s}_{\perp}. \quad (4.2)$$

Recalling that  $\boldsymbol{\epsilon}^{\pm}(\mathbf{s}) = (1/\sqrt{2})(\hat{\mathbf{e}}_{\perp}(\mathbf{s}), \pm i\hat{\mathbf{e}}_{\parallel}(\mathbf{s}), 0)$ , and writing in the Cartesian basis  $\hat{\mathbf{x}}, \hat{\mathbf{y}}, \hat{\mathbf{z}}$ , (see Fig. 1):  $\hat{\mathbf{e}}_{\perp}(\mathbf{s}) = (\sin \phi, \cos \phi, 0)$ ,  $\hat{\mathbf{e}}_{\parallel}(\mathbf{s}) = (\cos \theta \cos \phi, \cos \theta \sin \phi, -\sin \theta)$ ,

$$\mathbf{s} = (\sin \theta \cos \phi, \sin \theta \sin \phi, \cos \theta), \quad d^2 \mathbf{s}_{\perp} = d\Omega = \sin \theta \cos \theta d\theta d\phi. \quad 0 \leq \theta \leq \pi, \quad 0 \leq \phi \leq 2\pi$$

Performing the  $\phi$  and  $\theta$  integrals we obtain (see integrals 3.937.2 and 6.631.1 of [36]) after making  $\cos \theta \simeq 1$  in all factors of the integrand but not in the exponentials as involved in the paraxial approximation, and writing  $x + iy = R \exp(i\Phi)$ ,  $\Phi$  being the azimuthal angle, we derive:

$$\begin{aligned} \mathbf{E}(\mathbf{r}) = \frac{W_0^2}{4\sqrt{\pi}\sigma^3} e^{ikz} \left\{ \frac{R}{2} {}_1F_1\left(\frac{3}{2}; 2; -\frac{R^2}{2\sigma^2}\right) [-e_0^+ \exp(-i\Phi)(\hat{\mathbf{x}} + i\hat{\mathbf{y}}) + e_0^- \exp(i\Phi)(\hat{\mathbf{x}} - i\hat{\mathbf{y}})] \right. \\ \left. + \frac{i}{k} (e_0^+ - e_0^-) {}_1F_1\left(\frac{3}{2}; 1; -\frac{R^2}{2\sigma^2}\right) \hat{\mathbf{z}} \right\}. \end{aligned} \quad (4.3)$$

${}_1F_1$  is Kummer's confluent hypergeometric function [37].  $\sigma^2 = W_0^2/2 + iz/k$ . Eq. (4.3) represents a hypergeometric beam which, containing LCP and RCP plane waves, differs from some previously put forward [38]. A generalization of this beam to arbitrary index  $m$  with vortices  $\exp(\pm im\Phi)$  and topological charge  $m$  is made by including a factor  $\exp(-im\phi)$  in  $\mathbf{e}(\mathbf{s}_{\perp})$ . Notice from (4.3) that due to the paraxial approximation the transversal  $XY$ -component of  $\mathbf{E}$  is the sum of two fields [cf. Eq. (2.7)]: one,  $\mathbf{E}^+$ , is LCP and has a complex amplitude proportional to  $-e_0^+$ ; the other,  $\mathbf{E}^-$ , is RCP and its amplitude factors  $e_0^-$ . These two CPL beams also have a longitudinal component  $E_z$ , proportional to  $(i/k)e_0^+$  and  $-(i/k)e_0^-$ , respectively, as shown by the last term of (4.3). Next we see the relevance of this longitudinal component to control the dipole emission, enhancing the rate of either helicity or energy extinction. Using (4.3) we obtain for the incident energy and helicity factors in the left side of (3.6) and (3.7) [we now drop the subindex  $i$  in those equations, understanding that the incident electric field is (4.3)]:

$$|\mathbf{E}^+(\mathbf{r})|^2 \pm |\mathbf{E}^-(\mathbf{r})|^2 = \frac{W_0^4}{16\pi\sigma^6} (|e_0^+|^2 \pm |e_0^-|^2) \left[ \frac{R^2}{2} {}_1F_1^2\left(\frac{3}{2}; 2; -\frac{R^2}{2\sigma^2}\right) + \frac{1}{k^2} {}_1F_1^2\left(\frac{3}{2}; 1; -\frac{R^2}{2\sigma^2}\right) \right]. \quad (4.4)$$

Of course the choice of the upper or lower sign in  $\pm$  of (4.4) yields the beam energy or the helicity [cf. Eq. (2.12)], respectively.

Fig. 2 shows the transversal intensity distribution  $|\mathbf{E}^+|^2 + |\mathbf{E}^-|^2$  of this beam, given by Eq. (4.4) at  $z = 0$ , for  $e_0^- = ae_0^+ \exp(ib\pi/2)$ ,  $b$  real,  $e_0^+ = 1$  (in arbitrary units)  $a = 1$ ,  $\lambda = 589$  nm,  $W_0 = 4\lambda$ . This choice of the value of  $e_0^+$  and the presence of the factor  $W_0^2/4\sqrt{\pi}\sigma^3$  of the beam amplitude in (4.2) produces small values of these intensities. Also since  $R^2 \gg \lambda^2$ , apart from points close to  $R = 0$  the second term of (4.4), given by the longitudinal component of the beam, hardly contributes to this intensity distribution. However as seen next, this longitudinal component becomes crucial when the helicity, extinguished from the incident beam and thus radiated or scattered -or absorbed or converted [21]- by the particle, is considered. For comparison, we also show this intensity distribution when the  ${}_1F_1$  functions of (4.4) are

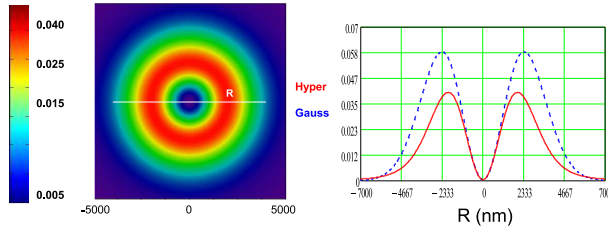


**Figure 2.** (Color online). Intensity  $|\mathbf{E}^+|^2 + |\mathbf{E}^-|^2$ , [cf. Eq. (4.4)], at  $z = 0$  of the hypergeometric beam of Eq. (4.3). Left: Color map of the transversal distribution. Right: a cut of this spatial distribution as a function of the coordinate  $R$  along a diameter, (full red). The distribution when the  ${}_1F_1$  functions are replaced by a Gaussian of the same  $\sigma$ , is also shown, (broken blue line).

substituted by a Gaussian with the same value of  $\sigma^2$ . The difference between both distributions is small due to the similar shapes of the Gaussian and these hypergeometric functions.

On the other hand, the real (and imaginary) part of the product  $\mathbf{E}^- \cdot \mathbf{E}^+$  reduces to:

$$\left\{ \begin{array}{c} \Re \\ \Im \end{array} \right\} [\mathbf{E}^- \cdot \mathbf{E}^+^*] = \left\{ \begin{array}{c} \Re \\ \Im \end{array} \right\} [E_z^- \cdot E_z^+^*] = -\frac{W_0^4}{16\pi\sigma^6 k^2} \left\{ \begin{array}{c} \Re \\ \Im \end{array} \right\} [e_0^- e_0^+^*] {}_1F_1\left(\frac{3}{2}; 1; -\frac{R^2}{2\sigma^2}\right). \quad (4.5)$$

So that either of these quantities,  $\Re[\cdot]$  or  $\Im[\cdot]$ , may be made arbitrarily small (or zero) depending on the choice of parameters  $e_0^-$  and  $e_0^+$  for the beam, which may make arbitrarily small (or zero)

the factor  $\left\{ \begin{array}{c} \Re \\ \Im \end{array} \right\} [e_0^- e_0^+^*]$ . In the next section we show the relevance of this choice in connection with Eqs.(3.6) and (3.7). For example, choosing like for Fig. 2:  $e_0^-/e_0^+ = \pm a \exp(ib\pi/2)$ ,  $a$  and  $b$  being real, the value of  $\left\{ \begin{array}{c} \Re \\ \Im \end{array} \right\} [\mathbf{E}^- \cdot \mathbf{E}^+^*]$  will oscillate as  $\mp \left\{ \begin{array}{c} \cos(b\pi/2) \\ \sin(b\pi/2) \end{array} \right\}$ , thus possessing several zero values in the interval  $0 \leq b \leq 4$ .

Notice that a kind of Hermite and Laguerre Gaussian beam modes  $(m, n)$  are straightforwardly worked out from (4.3) on making upon  $\mathbf{E}(\mathbf{r})$  the operations:  $\partial_x^m \partial_y^n$  and  $(\partial_x + i\partial_y)^m (\partial_x - i\partial_y)^{m+n}$ , respectively [35]. Likewise, Bessel beams with LCP and RCP angular components may be described by Eq. (4.2) using an angular spectrum:  $\delta(\mathbf{s} - \mathbf{s}_0)[e_0^+(\hat{\epsilon}_\perp(\mathbf{s}) + i\hat{\epsilon}_\parallel(\mathbf{s})) + e_0^-(\hat{\epsilon}_\perp(\mathbf{s}) - i\hat{\epsilon}_\parallel(\mathbf{s}))]$ .

## 5. Example: Enhancing the emission of either chirality or energy

As an illustration of the relevance of Eqs. (3.6) and (3.7), we consider a helical molecule with  $\alpha_e^R = 1.04 \times 10^{-2} \text{ nm}^3$ ,  $\alpha_{me}^I = 6.2 \times 10^{-5} \text{ nm}^3$ ,  $\alpha_{me}^R = 0$ , in an environment with  $\epsilon = \mu = 1$  at an illumination wavelength  $\lambda = 589 \text{ nm}$ .  $\alpha_e^I = (2/3)(2\pi/\lambda)^3 (\alpha_e^R)^2 \simeq 0.96 \cdot 10^{-10} \text{ nm}^3 \ll \alpha_e^R$ ,  $|\alpha_m| < 10^{-5} |\alpha_e|$  [19,39].

These polarizabilities yield according to (3.6) and (3.7) for the helicity extinction  $\mathcal{W}_{\mathcal{H}}^s$ :

$$\frac{\mu}{2\pi c} \mathcal{W}_{\mathcal{H}}^s \simeq (\alpha_e^I + \alpha_m^I)(|\mathbf{E}_i^+|^2 - |\mathbf{E}_i^-|^2) + 2(\alpha_e^R - \alpha_m^R) \Im[\mathbf{E}_i^- \cdot \mathbf{E}_i^+^*]; \quad (5.1)$$

and for the rate of energy extinction  $\mathcal{W}^s$ :

$$\frac{2}{\omega} \mathcal{W}^s \simeq (\alpha_e^I + \alpha_m^I)(|\mathbf{E}_i^+|^2 + |\mathbf{E}_i^-|^2) + 2(\alpha_e^I - \alpha_m^I) \Re[\mathbf{E}_i^- \cdot \mathbf{E}_i^+^*]. \quad (5.2)$$

We see from (5.1) that objects with such a purely imaginary  $\alpha_{me}$  would produce no signal in a standard circular dichroism configuration, i.e. under illumination with plane CPL waves, for which:  $|\mathbf{E}_i^+|^2 = |\mathbf{E}_i^-|^2$ ,  $\mathbf{E}^- \cdot \mathbf{E}^+^* = 0$ . (We recall that in such experiments the objects (molecules) usually have  $\alpha_{me}^R \leq 10^{-3} \alpha_e^I$ , but  $\alpha_{me}^R \neq 0$ ). However, impinging the particle by LCP and RCP

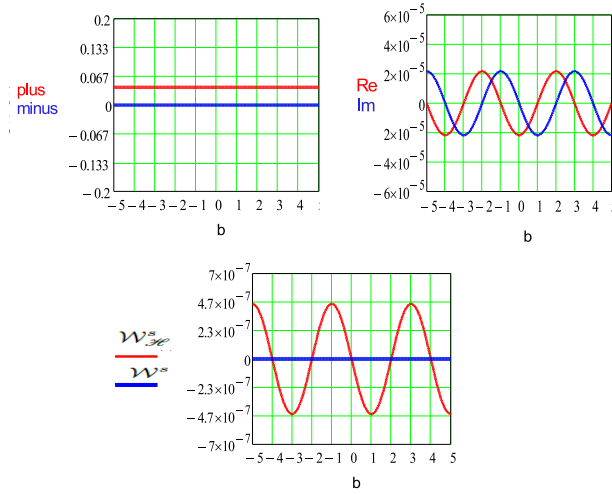


**Figure 3.** (Color online). Upper left: Intensity:  $plus = |\mathbf{E}^+|^2 + |\mathbf{E}^-|^2$  (red line) and helicity:  $minus = |\mathbf{E}^+|^2 - |\mathbf{E}^-|^2$  (blue line), [cf. Eq. (4.4)], as a function of  $b$  for the hypergeometric beam of Eq. (4.3) at  $z = 0$  and near the peak at:  $R = 2000$  nm, (see Fig. 2, right).  $e_0^- = ae_0^+ \exp(i b \pi / 2)$ ,  $e_0^+ = 1$  (in arbitrary units),  $a = 1$ . Upper right:  $Re = \Re[\mathbf{E}^- \cdot \mathbf{E}^+^*]$  and  $Im = \Im[\mathbf{E}^- \cdot \mathbf{E}^+^*]$ , [cf Eq. (4.5)], for the same beam and choice of parameters. Lower middle: Rate of helicity extinction  $\mathcal{W}_{\mathcal{H}}^s$  (full red) and energy extinction  $\mathcal{W}^s$  (broken blue) in terms of  $b$ .

beams with longitudinal component, like those of Eq. (4.3), and for example choosing as above:  $e_0^-/e_0^+ = \pm a \exp(i b \pi / 2)$ , Fig. 3 shows, at  $R = 2000$  nm and  $z = 0$ ,  $|\mathbf{E}_i^+|^2 \pm |\mathbf{E}_i^-|^2$ , as well as  $\Re$  (and  $\Im$ ) of  $[\mathbf{E}_i^- \cdot \mathbf{E}_i^+^*]$  as functions of  $b$  for  $W_0 = 4\lambda$ ,  $a = 1$ . The incident helicity, given by the quantity  $minus$  of Fig. 3, is zero since  $|\mathbf{E}_i^+|^2 = |\mathbf{E}_i^-|^2$ . As seen, the oscillations of the term  $2(\alpha_e^R - \alpha_m^R) \Im[\mathbf{E}_i^- \cdot \mathbf{E}_i^+^*]$  of (5.1) and of  $2(\alpha_e^I - \alpha_m^I) \Re[\mathbf{E}_i^- \cdot \mathbf{E}_i^+^*]$  of (5.2) lead to those of the helicity  $\mathcal{W}_{\mathcal{H}}^s$  and energy  $\mathcal{W}^s$  extinction rate, respectively. The latter is constantly zero due to the very small value of the factor  $(\alpha_e^I - \alpha_m^I)$  for these polarizabilities.

The corresponding quotient between  $\mathcal{W}_{\mathcal{H}}^s$  and  $\mathcal{W}^s$  would be very large in this case. Therefore this is just an illustration of how such a ratio may be enhanced depending on the constitutive parameters of the particle and choice of the beam. Other objects with different values of the polarizabilities may yield similar enhancements of either the extinguished helicity -chirality- or energy depending on whether  $\Im[\mathbf{E}_i^- \cdot \mathbf{E}_i^+^*]$  dominates upon  $\Re[\mathbf{E}_i^- \cdot \mathbf{E}_i^+^*]$  in (3.6) and (3.7), or viceversa. For instance, were the "particle" magnetodielectric with  $\alpha_m^I$  comparable to  $\alpha_e^R$ , or just one or two orders of magnitude smaller, (a difficult case to deal with conventional circular dichroism [22]), the factor  $2(\alpha_e^I - \alpha_m^I) \Re[\mathbf{E}_i^- \cdot \mathbf{E}_i^+^*]$  will give rise to an amplitude of the oscillations in  $\mathcal{W}^s$  comparable to that in  $\mathcal{W}_{\mathcal{H}}^s$ , or one or two orders of magnitude lower. However, the phase shift of the oscillations of  $\Re[\mathbf{E}_i^- \cdot \mathbf{E}_i^+^*]$  and  $\Im[\mathbf{E}_i^- \cdot \mathbf{E}_i^+^*]$ , (cf.  $Re$  and  $Im$  in Fig. 3), allows us to tailor the beam, producing an enhancement of  $\mathcal{W}_{\mathcal{H}}^s$  or of  $\mathcal{W}^s$ .

## 6. Concluding remarks

Based on a recent optical theorem put forward for the electromagnetic helicity -or chirality- extinction rate in quasimonochromatic wavefields [16], we have demonstrated that dichroism is not only a manifestation of molecular absorption, but it is a universal phenomenon which appears in the scattering -or diffraction- of twisted waves. This provides a general basic answer to the question on the conditions under which an object produces chiral fields and/or dichroism, and whether a chiral scatterer is required to produce such effect.

In this respect we have established that both dichroism and chirality of emitted or scattered wavefields from wide sense dipolar particles are consequences of the helicity of the illumination, or of the mutual relationship between the emitting electric and magnetic dipoles; but these phenomena do not require the object constitutive parameters, refractive indices and polarizabilities, to be those of a chiral structure. For example, as we have shown, to obtain a circularly polarized emitted or scattered field, it is a sufficient condition that the particle induced electric and magnetic dipoles rotate and differ from each other by only a  $\pm\pi/2$  phase; but no chiral cross-polarizability  $\alpha_{me}$  is necessary. Thus an achiral particle ( $\alpha_{me} = 0$ ) may produce dichroism on scattering of a chiral incident wave. Henceforth the standard concept of circular dichroism is generalized to include fields with both LCP and RCP components and a net helicity.

Based on the angular spectrum representation we have introduced new families of optical beams with right circular and left circular polarization, and with longitudinal components. Tailoring these fields, used in our optical theorem as incident waves on the scattering particle, overcomes previous limitations of circular dichroism without needing to place nearby additional objects to enhance the signal [28,29,40]. Depending on the parameters chosen for these beams, the enhancement of the extinction rate of helicity and/or of energy is produced, i.e. the dichroism scattered signal is either augmented or lowered. This not only provides a new procedure for object (and particularly enantiomeric) characterization on illumination with twisted beams, but it also yields a way of controlling the helicity and energy of radiated wavefields by using such scattering particles as secondary sources.

## References

1. Richardson, F.S. and Riehl, J.P. 1977 Circularly Polarized Luminescence Spectroscopy, Chem. Rev. **77**, 773-792.
2. Allen, L., Barnett S. M. and Padgett, M. J. , eds 2003 *Optical Angular Momentum*, (IOP Publishing, Bristol.
3. Allen, L., Padgett M. J. and Babiker M., The orbital angular momentum of light. In *Prog. Opt.* **39**, E. Wolf, ed., (Elsevier, Amsterdam, 1999).
4. Y. Tang and A. E. Cohen 2010, Optical Chirality and Its Interaction with Matter, Phys. Rev. Lett. **104**, 163901.
5. Y. Tang and A. E. Cohen 2011, Enhanced Enantioselectivity in Excitation of Chiral Molecules by Superchiral Light, Science **332**, 333-336.
6. Cameron, R. P, Barnett, S.M and Yao, A. M. 2012, Optical helicity, optical spin and related quantities in electromagnetic theory New. J. Phys. **14**, 053050 1-16.
7. Riehl J. P. and Muller G. 2012 Circularly polarized luminescence spectroscopy and emission-detected circular dichroism. In *Comprehensive Spectroscopy*, Vol. 1. , Ch. 3., N. Berova, P. L. Polavarapu, K. Nakanishi and R. W. Woody, eds., J. Wiley, New Jersey.
8. Andrews, D. L. and Babiker, M. eds. 2013 *The Angular Momentum of Light*(Cambridge University Press, Cambridge.
9. Cameron, R.P., ÅG Gotte, J.B. Barnett, S.M. 2015, Chiral Rotational Spectroscopy, arXiv:1511.04615v1.
10. Andrews, D. L. and Coles, M. M. 2012, Photonic measures of helicity: optical vortices and circularly polarized reflection , Opt.Lett. **38**, 869-871.
11. Andrews, D. L., Coles, M. M., Williams M. D. and Bradshaw, D. S. 2013, Expanded horizons for generating and exploring optical angular momentum in vortex structures Proc. SPIE **8813**, 88130Y .
12. O'Sullivan, M. N., Mirhosseini, M., Malik M. and Boyd, R. W. 2012, Near-perfect sorting of orbital angular momentum and angular position states of light, Opt. Express **20**, 24444-24449.
13. Krenn, M., Tischler, N. and Zeilinger, A. 2016, On Small Beams with Large Topological Charge, New. J. Phys. **18**, 033012 - 033019.
14. Lipkin, D.M. 1964, Existence of a New Conservation Law in Electromagnetic Theory, J. Math. Phys. **5** , 696-700.
15. Bliokh, K. Y. and Nori, F. 2011, Characterizing optical chirality, Phys. Rev. A. **83** 021803(R) 1-3.
16. Nieto-Vesperinas, M. 2015, Optical theorem for the conservation of electromagnetic helicity: Significance for molecular energy transfer and enantiomeric discrimination by circular dichroism, Phys. Rev. A **92**, 023813 1-8.

17. Schellman, J. A. (1975), Circular Dichroism and Optical Rotation, *Chem. Rev.* **75**, 323-331.
18. Craig, D. P. and Thirunamachandran, T. 1998, *Molecular Quantum electrodynamics: An Introduction to Radiation Molecule Interactions*, Dover, New York.
19. Barron, L. D. 2004, *Molecular Light Scattering and Optical Activity*, Cambridge University Press, Cambridge.
20. Zambrana-Puyalto, X., Vidal, X. and Molina-Terriza, G. 2014, Angular momentum-induced circular dichroism in non-chiral nanostructures, *Nature Comm.* **5** 4922.
21. Poulikakos, L. V., Gutsche, P., McPeak, K. M., Burger, S., Niegemann, J., Hafner, C. and Norris, D. J. 2016, The optical chirality flux as a useful far-field probe of chiral near fields, arXiv:1601.06716v1. Gutsche, P., Poulikakos, L.V., Hammerschmidt, M., Burger, S. and Schmidt, F. 2016, Time-harmonic optical chirality in inhomogeneous space, arXiv:1603.05011v1.
22. Choi, J. S. and Cho, M. 2012, Limitations of a superchiral field, *Phys. Rev. A* **86**, 063834 1-22.
23. Kong, J.A. 1972, *Proc IEEE* **60**, Theorems of bianisotropic Media, 1036-1046.
24. Nieto-Vesperinas, M. 2015, Optical torque: Electromagnetic spin and orbital-angular-momentum conservation laws and their significance, *Phys. Rev. A* **92**, 043843 1-18.
25. Bohren, C. F. and Huffman, D.R. 1983, *Absorption and Scattering of Light by Small Particles*, J. Wiley, New York.
26. Born, M. and Wolf, E. 1999 *Principles of Optics*, 7 th edition, Cambridge University Press, Cambridge.
27. L. Novotny and B. Hecht 2012, *Principles of Nano-Optics*, 2nd edition, Cambridge University Press, Cambridge.
28. Guzatov, D. V. and Klimov, V.V. 2012, The influence of chiral spherical particles on the radiation of optically active molecules, *New J. Phys.* **14**, 123009 1-19.
29. Alaeian, H. and Dionne, J. A. 2015, Controlling electric, magnetic, and chiral dipolar emission with PT-symmetric potentials, *Phys. Rev. B* **91**, 245108 1-8.
30. Jackson, J. D. 1998, *Classical Electrodynamics*, 3rd edition, John Wiley, New York.
31. Mandel, L. and Wolf, E. 1995, *Optical Coherence and Quantum Optics*, Cambridge University press., Cambridge.
32. Nieto-Vesperinas, M. 2006, *Scattering and Diffraction in Physical Optics*, 2nd edition, World Scientific, Singapore.
33. J. Crichton, H. and . Marston, P. L. 2000, The measurable distinction between the spin and orbital angular momenta of electromagnetic Radiation, *Electron. J. Dif. Eqs.*, **Conf. 04**, 37 . <http://ejde.math.swt.edu> or <http://ejde.math.unt.edu>.
34. Berry, M.V. 2009, Optical currents, *J. Opt. A* **11**, 094001- 094012.
35. Zauderer, E. 1986, Complex argument Hermite-Gaussian and Laguerre-Gaussian beams, *J. Opt. Soc. Am. A* **3**, 465-469.
36. Gradshteyn, I. S. and Ryzhik, I. M. 2007, *Table of Integrals, Series, and Products*. Edited by Alan Jeffrey, A. and Zwillinger, D., 7th Edition, Academic Press, New York.
37. Abramowitz, M. and Stegun, I. 1972, *Handbook of mathematical Functions* , National Bureau of Standards, Applied Mathematical Series Vol. 25, 3rd Printing, Washington D.C.
38. Karimi, E., Zito, G., Piccirillo, B., Marrucci, L. and Santamato. E. 2007, Hypergeometric-gaussian modes , *Opt. Lett.* **32**, 3053-3055.
39. Hayat, A., Mueller, J. P. B., and Capasso, F. 2016 , Lateral chirality-sorting optical forces, *Proc. Nat. Acad. Sci.* **112**, 13190-13194.
40. Krasnok, A., Glybovski, S., Petrov, M. Makarov, S., Savelev, R., Belov, P., Simovski, C. and Kivshar, Y. 2016, Demonstration of the enhanced Purcell factor in all-dielectric structures, arXiv:1606.00477v1.

**Data Accessibility.** This research involves no data.

**Funding.** Work supported by MINECO, grants FIS2012-36113-C03-03, FIS2014-55563-REDC and FIS2015-69295-C3-1-P.

**Acknowledgements.** The author thanks Dr. J. M. Auñón for a critical reading of the manuscript and helpful comments